Available online at www.sciencedirect.com

ScienceDirect

IFAC PapersOnLine 56-2 (2023) 6423–6428

Finite Dimensional Koopman Form of Polynomial Nonlinear Systems[★]

Lucian C. Iacob[*] Maarten Schoukens[*] Roland Tóth[*,**]

[*] *Control Systems Group, Eindhoven University of Technology, Eindhoven, The Netherlands*
e-mail: l.c.iacob@tue.nl, m.schoukens@tue.nl, r.toth@tue.nl
[**] *Systems and Control Laboratory, Institute for Computer Science and Control, Budapest, Hungary*

Abstract: The Koopman framework is a popular approach to transform a finite dimensional nonlinear system into an infinite dimensional, but linear model through a lifting process using so-called observable functions. While there is an extensive theory on infinite dimensional representations in the operator sense, there are few constructive results on how to select the observables to realize them. When it comes to the possibility of finite Koopman representations, which are highly important from a practical point of view, there is no constructive theory. Hence, in practice, often a data-based method and ad-hoc choice of the observable functions is used. When truncating to a finite number of basis, there is also no clear indication of the introduced approximation error. In this paper, we propose a systematic method to compute the finite dimensional Koopman embedding of a specific class of polynomial nonlinear systems in continuous-time, such that the embedding can fully represent the dynamics of the nonlinear system without any approximation.

Keywords: Nonlinear systems, Koopman operator, Linear embedding

1. INTRODUCTION

In most engineering fields, due to increasing performance demands, tackling the nonlinear behaviour becomes more and more important. However, the available methods in the field of nonlinear control (e.g. feedback linearization, backstepping, sliding mode control (Khalil, 2002)) are generally complex to design, only offer stability guarantees, and offer limited capeabilites for performance shaping. This is in contrast to the systematic and powerful tools available for *linear time invariant* (LTI) systems. However, using LTI control methods designed for a linearized model of the original nonlinear plant around an operating point offers good local performance only in the neighborhood of the operating point, which neighborhood can be arbitrary small. Hence, there is an increasing need to extend the powerful LTI control design and modelling framework to address nonlinear systems beyond local control. As such, there is a significant interest in finding globally linear surrogate models of nonlinear systems.

One of the more promising approaches to achieve this is the Koopman framework (Mauroy et al., 2020), (Bevanda et al., 2021), where the concept is to project the original nonlinear state space to a higher dimensional (possibly infinite), but linear space, through observable functions. For this space, a linear Koopman operator exists to describe the original nonlinear dynamics through the observables. The Koopman framework shows promising results in its application to real-world analysis and control applications (e.g. mechatronic systems (Abraham and Murphey, 2019), (Cisneros et al., 2020), distributed parameter systems (Klus et al., 2020)). For practical use, a finite number of observables needs to be selected, which is called the lifting. Based on these, time-shifted data matrices are constructed to compute via least-squares a matrix approximation of the Koopman operator. This technique is known as *extended dynamic mode decomposition* (EDMD) (Williams et al., 2015). However, the main problem is that the choice of the observables is heuristic and there are no guarantees on the quality of the resulting model. To tackle this, one solution is to use data-driven techniques to learn the lifting from data, in order to circumvent the manual selection of observables (Lusch et al., 2018), (Iacob et al., 2021). Nevertheless, this is still an approximation and the questions on how to embed the nonlinear system into an exact linear finite dimensional lifted representation and when this is possible at all are still open. This is an important aspect, because, for control purposes, having an exact finite dimensional embedding allows for the application of the available control tools for linear systems. Moreover, if there exist approximation errors in the model that cannot be quantified, the expected performance will not be achieved. To tackle this, there have been attempts to connect the Koopman framework to immersion (Wang and Jungers, 2020) and Carleman linearization, in order to obtain a clear way of computing the observables. However, in the immersion approach, the existence of a finite dimensional fully linear lifting depends heavily on the observability property of the system and, in general, the resulting embedding contains a nonlinear output injection (Krener and Isidori, 1983), (Jouan, 2003). Closely connected to the

[★] This work has received funding from the European Research Council (ERC) under the European Union's Horizon 2020 research and innovation programme (grant agreement nr. 714663) and from the European Union within the framework of the National Laboratory for Autonomous Systems (RRF-2.3.1-21-2022-00002).

10.1016/j.ifacol.2023.10.849

immersion approach is the notion of polyflows, which allow for a finite linear embedding of the system through the Lie derivatives of the trajectories. However, the corresponding polyflow property can only be satisfied in an approximate sense for general nonlinear systems and the approach is non-constructive in terms of the resulting Koopman form, which is still obtained via a data-driven approximation (Jungers and Tabuada, 2019). Regarding the Carleman linearization (Kowalski and Steeb, 1991), while it offers a systematic way of computing the lifting functions, the resulting embedding is still an infinite dimensional model that needs to be trimmed.

The present paper discusses a novel method to systematically convert a polynomial nonlinear system to an exact finite dimensional linear embedding and compute the corresponding linear representation analytically (without EDMD). Starting from the idea of the simple 2-dimensional example shown in (Brunton et al., 2022), we introduce a state-space model where the state equation is described by a lower triangular polynomial form. We prove that there always exists an exact finite dimensional Koopman representation and we show how to systematically compute it. This approach is applicable for the class of nonlinear systems for which there exists a bijective nonlinear state transformation that brings the state-space description of the system to this lower triangular form. We also show that, once the autonomous part of the nonlinear system is embedded, the extension to systems with inputs is trivial and can be performed in a separate step. Using an example system, we demonstrate that the lifted Koopman model can fully capture the original dynamics, both in an autonomous operation and in the presence of inputs.

The paper is structured as follows. Section 2 describes the Koopman framework and details the proof and steps needed to obtain the finite embedding. In Section 3, we discuss the example and showcase the simulation results. In Section 4, conclusions on the presented results are given together with outlooks on future research.

2. FINITE DIMENSIONAL EMBEDDING

The present section details the Koopman framework and introduces the proposed method to compute an exact finite dimensional embedding. Additionally, we discuss the extension to systems with inputs.

2.1 Koopman framework

Consider the autonomous nonlinear system:

$$\dot{x} = f(x), \tag{1}$$

with $x := x(t)$ denoting the state, $t \in \mathbb{R}$ represents the time and $f : \mathbb{R}^{n_\mathrm{x}} \to \mathbb{R}^{n_\mathrm{x}}$ is the nonlinear vector field which we consider to be a Lipshitz continuous function. Given an initial condition $x(0) \in \mathbb{X} \subseteq \mathbb{R}^{n_\mathrm{x}}$, the solution $x(t)$ can be described as:

$$x(t) = F(t, x(0)) := x(0) + \int_0^t f(x(\tau))\,\mathrm{d}\tau. \tag{2}$$

It is assumed that $\mathbb{X}$ is compact and forward invariant under the flow $F(t,\cdot)$, such that $F(t,\mathbb{X}) \subseteq \mathbb{X}, \forall t \geq 0$. Introduce the family of Koopman operators $\{\mathcal{K}^t\}_{t\geq 0}$ associated to the flow $F(t,\cdot)$ as:

$$\mathcal{K}^t \phi(x(0)) = \phi \circ F(t, x(0)), \quad \phi \in \mathcal{F}, \tag{3}$$

where $\mathcal{F} \subseteq \mathcal{C}^1$ is a Banach function space of continuously differentiable functions and $\phi : \mathbb{X} \to \mathbb{R}$ is a scalar observable function. As the flow F is uniformly Lipshitz and $\mathbb{X}$ is compact forward-invariant, the Koopman semigroup $\{\mathcal{K}^t\}_{t\geq 0}$ is strongly continuous on $\mathcal{F}$ (Mauroy et al., 2020). Thus, the infinitesimal generator $\mathcal{L} : \mathcal{D}_\mathcal{L} \to \mathcal{F}$ associated with $\{\mathcal{K}^t\}_{t\geq 0}$ can be described as (Lasota and Mackey, 1994; Mauroy et al., 2020):

$$\mathcal{L}\phi(x_0) = \lim_{t\downarrow 0} \frac{\mathcal{K}^t\phi(x(0)) - \phi(x(0))}{t}, \quad \phi \in \mathcal{D}_\mathcal{L}, \tag{4}$$

where $\mathcal{D}_\mathcal{L}$ is a dense set in $\mathcal{F}$. Note that, as described in (Lasota and Mackey, 1994), the generator $\mathcal{L}$ is a linear operator. Through the infinitesimal generator, we can thus describe the dynamics of observables as follows:

$$\dot{\phi} = \frac{\partial \phi}{\partial x} f = \mathcal{L}\phi, \tag{5}$$

which is a linear infinite dimensional representation of the nonlinear system (1). If there exists a finite dimensional Koopman subspace $\mathcal{F}_{n_\mathrm{f}} \subseteq \mathcal{D}_\mathcal{L}$, such that the image of $\mathcal{L}$ is in $\mathcal{F}_{n_\mathrm{f}}$, then, given the set of lifting functions as basis of $\mathcal{F}_{n_\mathrm{f}}$, we have $\mathcal{L}\phi \in \mathrm{span}\{\Phi\}$, $\forall \phi \in \Phi$. Thus, the following relation holds:

$$\dot{\phi}_j = \mathcal{L}\phi_j = \sum_{i=1}^{n_\mathrm{f}} L_{i,j}\phi_i, \tag{6}$$

where L denotes the matrix representation of $\mathcal{L}$ and the coordinates of $\mathcal{L}\phi_j$ in the basis Φ are contained in the column $L_{\bullet,j}$ Let $A = L^\top \in \mathbb{R}^{n_\mathrm{f}\times n_\mathrm{f}}$, then, based on (5), the lifted representation of (1) is given by:

$$\dot{\Phi}(x) = \frac{\partial \Phi}{\partial x}(x) f(x) = A\Phi(x). \tag{7}$$

Thus, one can formulate conditions for the existence of a finite dimensional embedding of (1) as:

$$\dot{\Phi} \in \mathrm{span}\{\Phi\}, \tag{8a}$$

which is equivalent to

$$\frac{\partial \Phi}{\partial x} f \in \mathrm{span}\{\Phi\}. \tag{8b}$$

However, the major question is how to compute Φ such that the conditions (8) are true. In the Koopman framework, to recover the original states of (1), the existence of a back transformation $\Phi^\dagger(\Phi(x)) = x$ is often assumed. For simplicity, this is achieved by adding an extra condition to (8), namely that the original states are contained in Φ, i.e., the identity function is part of Φ. Next, in order to explicitly write the LTI dynamics given by the Koopman form, let $z(t) = \Phi(x(t))$. Then, an associated Koopman representation of (1) is:

$$\dot{z} = Az, \quad \text{with } z(0) = \Phi(x(0)). \tag{9}$$

It is important to note that, by the existing theory, in general, one cannot guarantee the existence of a finite dimensional Koopman invariant subspace $\mathcal{F}_{n_\mathrm{f}}$. In the sequel, we show that, in case of systems described by a state-space representation where the state equation can be written in a lower triangular polynomial form, there always exists an exact finite dimensional Koopman representation of the system in the form of (9) and this representation can be systematically computed.

2.2 Exact finite embedding procedure

We assume the existence of a bijective nonlinear state transformation $\Psi : \mathbb{R}^{n_\mathrm{x}} \to \mathbb{R}^{n_\mathrm{x}}$ such that $\frac{\mathrm{d}}{\mathrm{d}t}\Psi(x) = f(\Psi(x))$ results in the following equivalent state-space representation of the original system:

$$
\begin{aligned}
\dot{x}_1 &= a_1 x_1 \\
\dot{x}_2 &= a_2 x_2 + f_2(x_1) \\
\dot{x}_3 &= a_3 x_3 + f_3(x_1, x_2) \\
&\ \vdots \\
\dot{x}_n &= a_n x_n + f_n(x_1, \dots, x_{n-1})
\end{aligned} \tag{10}
$$

where f_p (with $p \in \{2, \dots, n\}$) is given by:

$$
f_p(x_1, \dots, x_{p-1}) = \sum_{j_1=0}^{d_p} \cdots \sum_{j_{p-1}=0}^{d_p} \alpha^{(p)}_{j_1 \cdots j_{p-1}} \prod_{i=1}^{p-1} x_i^{j_i}, \tag{11}
$$

with polynomial terms of the form $x_1^{j_1} \dots x_{p-1}^{j_{p-1}}$. Here, as an abuse of notation, we do not distinguish the new state variable with a different notation such as $\tilde{x} = \Psi(x)$. Furthermore d_n is the maximum power of the resulting polynomial terms, hence for the generality of the notation we do not distinguish the minimal power of each subterm that results from such a conversion. Under these considerations, we can give the following theorem.

Theorem 1. For an autonomous continuous-time nonlinear system that has a polynomial state-space representation in the form of (10), there exists an exact finite-dimensional polynomial lifting $\Phi : \mathbb{R}^{n_\mathrm{x}} \to \mathbb{R}^{n_\mathrm{f}}$, containing the states x_i, with $i \in \{1, \dots, n\}$, such that (8a) holds true.

Proof. The theorem is proven by induction. First, we will consider the cases when $n = 1, 2, 3, 4$ and then we will show that if the statement of Theorem 1 holds for n-number of states then we can prove that it also holds for $n + 1$.

- $n = 1$: Consider the 1st-order system

  $$
  \dot{x}_1 = a_1 x_1 \tag{12}
  $$

  Let $W_1 = \{x_1\}$ and $\Phi = \mathrm{vec}(W_1)$, i.e., $\Phi(x) = x_1$. It is trivial to see that condition (8a) holds true as $\dot{x}_1 = a_1 x_1 \in \mathrm{span}\{\Phi\}$.
- $n = 2$: Notice that the dynamics defined by the 2nd-order system are described by (12), together with

  $$
  \dot{x}_2 = a_2 x_2 + \sum_{j_1=0}^{d_2} \alpha^{(2)}_{j_1} x_1^{j_1}. \tag{13}
  $$

  Here, superscript $^{(2)}$ of the coefficient α denotes that it belongs to the 2nd state equation. Let $V_2 = \{x_1^0, \dots, x_1^{d_2}\}$ and $W_2 = \{x_2\} \cup V_2$, while $\Phi = \mathrm{vec}(W_1 \cup W_2)$. By calculating $\dot{\Phi}$, we get the terms associated with W_1 and the terms

  $$
  \frac{\mathrm{d}}{\mathrm{d}t}\left(x_1^{j_1}\right) = j_1 x_1^{j_1-1} \dot{x}_1 = j_1 a_1 x_1^{j_1} \tag{14}
  $$

  originating from V_2. It is easy to observe that all terms in (14) are already contained in Φ and $\dot{x}_2 \in \mathrm{span}\{\Phi\}$, hence condition (8a) holds true.
- $n = 3$: The dynamics of the 3rd-order system are described by (12), (13) and the following equation:

  $$
  \dot{x}_3 = a_3 x_3 + \sum_{j_1=0}^{d_3} \sum_{j_2=0}^{d_3} \alpha^{(3)}_{j_1, j_2} x_1^{j_1} x_2^{j_2}. \tag{15}
  $$

  As performed previously, we take the nonlinear terms $x_1^{j_1} x_2^{j_2}$ and add them to the set of lifting functions $V_3 = \{x_1^0 x_2^0, \dots, x_1^{d_3} x_2^{d_3}\}$ and $W_3 = \{x_3\} \cup V_3$, while $\Phi = \mathrm{vec}(W_1 \cup W_2 \cup W_3)$. By calculating $\dot{\Phi}$, we get the terms associated with W_1, W_2 as before and

  $$
  \begin{aligned}
  \frac{\mathrm{d}}{\mathrm{d}t}\left(x_1^{j_1} x_2^{j_2}\right) &= j_1 x_1^{j_1-1} x_2^{j_2} \dot{x}_1 + j_2 x_1^{j_1} x_2^{j_2-1} \dot{x}_2 \qquad (16) \\
  &= (j_1 a_1 + j_2 a_2) \underbrace{x_1^{j_1} x_2^{j_2}}_{a} + j_2 \sum_{\tilde{j}_1=0}^{d_2} \alpha^{(2)}_{\tilde{j}_1} \underbrace{x_1^{j_1+\tilde{j}_1} x_2^{j_2-1}}_{b}
  \end{aligned}
  $$

  based on V_3. The following observations can be made:
  - The terms a are already contained in V_3.
  - For the terms b, we can observe that the power j_2 decreases by 1 and j_1 increases by at most d_2.

  Introduce the operator $\mathfrak{D}_\mathrm{b}$ such that $\mathfrak{D}_\mathrm{b}(x_1^{j_1} x_2^{j_2}) = \{x_1^{j_1+\tilde{j}_1} x_2^{j_2-1}\}_{\tilde{j}_1=0}^{d_2}$, i.e., it gives the b terms of (16). Then let $V_3 \leftarrow V_3 \cup \mathfrak{D}_\mathrm{b}(V_3)$. Repeating the process, i.e., applying the time derivative again to $x_1^{j_1+\tilde{j}_1} x_2^{j_2-1}$ further decreases j_2 and increases the power of x_1, and at each step only terms of the form a and b are generated. Repeating the process for a finite number of steps gives that $\mathfrak{D}_\mathrm{b}(V_3) \backslash V_3 \subseteq \{x_1^0, \dots, x_1^{n_1}\}$. Hence, based on case $n = 2$, we know that for $V_3 \leftarrow V_3 \cup \mathfrak{D}_\mathrm{b}(V_3)$ taking $W_3 = \{x_3\} \cup V_3$ and $\Phi = \mathrm{vec}(W_1 \cup W_2 \cup W_3)$ will ensure that condition (8a) holds true.
- $n = 4$: The dynamics of the 4th-order system is described by (12), (13), (15), together with:

  $$
  \dot{x}_4 = a_4 x_4 + \sum_{j_1=0}^{d_4} \sum_{j_2=0}^{d_4} \sum_{j_3=0}^{d_4} \alpha^{(4)}_{j_1, j_2, j_3} x_1^{j_1} x_2^{j_2} x_3^{j_3}. \tag{17}
  $$

  To ease readability, let $\zeta_j = x_1^{j_1} x_2^{j_2}$ with $j = j_1 + (d_4 + 1) j_2 + 1$. This means that $j = 1$ corresponds to $j_1 = 0, j_2 = 0$, $j = 2$ corresponds to $j_1 = 1, j_2 = 0$, up until $j = P = (d_4 + 1)^2$, which corresponds to $j_1 = d_4, j_2 = d_4$. Then, (17) can be written as

  $$
  \dot{x}_4 = a_4 x_4 + \sum_{j=1}^{P} \sum_{j_3=0}^{d_4} \tilde{\alpha}^{(4)}_{j, j_3} \zeta_j x_3^{j_3}. \tag{18}
  $$

  Let $V_4 = \{\zeta_1 x_3^0, \dots, \zeta_P x_3^{d_4}\}$ and $W_4 = \{x_4\} \cup V_4$, while $\Phi = \mathrm{vec}(\bigcup_{i=1}^4 W_i)$. By calculating $\dot{\Phi}$, we get the terms associated with W_1, W_2, W_3 as before and

  $$
  \begin{aligned}
  \frac{\mathrm{d}}{\mathrm{d}t}\left(\zeta_j x_3^{j_3}\right) &= \dot{\zeta}_j x_3^{j_3} + j_3 \zeta_j x_3^{j_3-1} \dot{x}_3 \qquad (19) \\
  &= j_3 a_3 \underbrace{\zeta_j x_3^{j_3}}_{a} + j_3 \sum_{\tilde{j}=1}^{P} \tilde{\alpha}^{(3)}_{\tilde{j}} \underbrace{\zeta_{j+n_{\tilde{j}}} x_3^{j_3-1}}_{b} + \underbrace{\dot{\zeta}_j x_3^{j_3}}_{c}
  \end{aligned}
  $$

  - The terms a are already contained in V_4.
  - For the terms b, we can observe that the power j_3 decreases by 1 and the powers of x_1 and x_2 within ζ increase by at most d_3 (which is finite), encoded in terms of $n_{\tilde{j}}$. Applying the same iterations as in case $n = 3$, we can construct a V_4 such that $\mathfrak{D}_\mathrm{b}(V_4) \setminus V_4 \subseteq \{\zeta_1, \dots, \zeta_{n_\zeta}\}$. We can observe that the ζ_j terms are in the form of the b terms in case of $n = 3$, hence the same procedure can be further applied till $\mathfrak{D}_\mathrm{b}(V_4) \setminus V_4 \subseteq \{x_1^0, \dots, x_1^{n_1}\}$.
  - For the terms c, $\frac{\mathrm{d}}{\mathrm{d}t}\zeta_j$ leads to a decrease of the orders of $x_1^{j_1}$ and $x_2^{j_2}$ in the terms ζ. Introduce the operator $\mathfrak{D}_\mathrm{c}$ such that $\mathfrak{D}_\mathrm{c}(\zeta_j x_3^{j_3}) = \{\dot{\zeta}_j x_3^{j_3}\}_{j=1}^{P}$, i.e., it gives the c terms of (19). Then let $V_4 \leftarrow V_4 \cup \mathfrak{D}_\mathrm{c}(V_4)$. Repeating the process for a finite number of steps gives that $\mathfrak{D}_\mathrm{c}(V_4) \setminus V_4 \subseteq \{x_1^0 x_3^0, \dots, x_1^{n_1} x_3^{n_3}\}$. Next, $\mathfrak{D}_b$ can be applied as

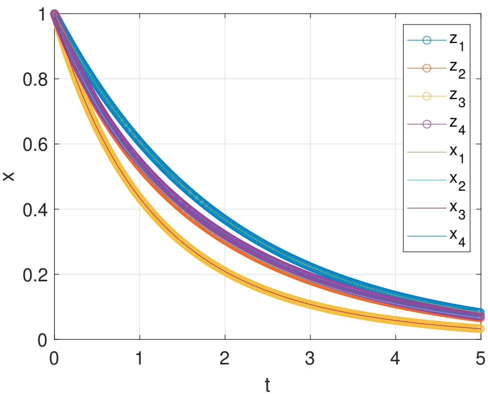

Fig. 1. State trajectories of the nonlinear system representation (29a)-(29d) and the Koopman embedding (30).

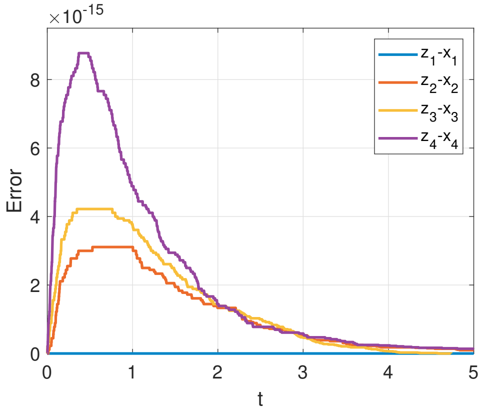

Fig. 2. Error between the state trajectories of the original nonlinear system representation (29a)-(29d) and the Koopman embedding (30).

$\mathfrak{D}_b(x_1^{j_1}x_3^{j_3}) = \{\zeta_{j+j_1}x_3^{j_3-1}\}_{j=1}^{P}$. This holds as the powers of both x_1 and x_2 increase through the application of $\mathfrak{D}_b$. Iterating both the b and c terms together leads to $\mathfrak{D}_{\mathrm{b}}(V_4) \setminus V_4 \subseteq \{x_1^0, \ldots, x_1^{n_1}\}$.

Hence, based on case $n = 3$, we know that for $V_4 \leftarrow V_4 \cup \mathfrak{D}_{\mathrm{b}}(V_4)$ taking $W_4 = \{x_4\} \cup V_4$ and $\Phi = \mathrm{vec}(\bigcup_{i=1}^{4} W_i)$ will ensure that condition (8a) holds true.

- $n+1$ states ($n+1$ order system):
  Assume that for $\Phi = \mathrm{vec}(\bigcup_{i=1}^{n} W_i)$, condition (8a) holds true in the n^{th}-order case. The dynamics of the $n+1$ order system is described by (10), together with:

$$\dot{x}_{n+1} = a_n x_n + \sum_{j_1=0}^{d_{n+1}} \cdots \sum_{j_n=0}^{d_{n+1}} \alpha_{j_1 \ldots j_n}^{(n+1)} x_1^{j_1} \ldots x_n^{j_n}. \tag{20}$$

Similar to the strategy in the $n = 4$ case, introduce $\zeta_j = x_1^{j_1} \ldots x_{n-1}^{j_{n-1}}$, with $j = 1 + \sum_{k=1}^{n-1} j_k(d_{n+1}+1)^{k-1}$ and $P = (d_{n+1}+1)^{n-1}$. With this notation, (20) reads as:

$$\dot{x}_{n+1} = a_{n+1}x_{n+1} + \sum_{j=1}^{P} \sum_{j_n=0}^{d_{n+1}} \tilde{\alpha}_{j,j_n}^{(n+1)} \zeta_j x_n^{j_n}. \tag{21}$$

Let $V_{n+1} = \{\zeta_1 x_n^0, \ldots, \zeta_P x_n^{d_{n+1}}\}$ and $W_{n+1} = \{x_{n+1}\} \cup V_{n+1}$, while $\Phi = \mathrm{vec}(\bigcup_{i=1}^{n+1} W_i)$. By calculating $\dot{\Phi}$, we get the terms associated with $W_1, \ldots, W_n$ as before and

$$\begin{aligned} \frac{\mathrm{d}}{\mathrm{d}t}\left(\zeta_j x_n^{j_n}\right) &= \dot{\zeta}_j x_n^{j_n} + j_n \zeta_j x_n^{j_n-1}\dot{x}_n \\ &= j_n a_n \underbrace{\zeta_j x_n^{j_n}}_{a} + j_n \sum_{\tilde{j}=1}^{P} \tilde{\alpha}_{\tilde{j}}^{(n)} \underbrace{\zeta_{j+n_{\tilde{j}}} x_n^{j_n-1}}_{b} + \underbrace{\dot{\zeta}_j x_n^{j_n}}_{c} \end{aligned} \tag{22}$$

· The terms a are already contained in W_n.

· We can observe that the power j_n decreases by 1 and the powers of x_i ($i \in \{1, \ldots, n-1\}$) within ζ increase by at most d_n (which is finite), encoded in terms of $n_{\tilde{j}}$. Applying the same iterations as in the previous cases, recursively leads to $\mathfrak{D}_{\mathrm{b}}(V_{n+1}) \setminus V_{n+1} \subseteq \{x_1^0, \ldots, x_1^{n_1}\}$ in a finite number of steps.

· As seen in the previous cases, taking $\frac{\mathrm{d}}{\mathrm{d}t}\zeta_j$ for the terms c, leads to a decrease of the orders of $x_1^{j_1}, \ldots, x_n^{j_n}$ in the terms ζ. By using $V_{n+1} \leftarrow V_{n+1} \cup \mathfrak{D}_{\mathrm{c}}(V_{n+1})$ in a finite number of steps leads to $\mathfrak{D}_{\mathrm{c}}(V_{n+1}) \setminus V_{n+1} \subseteq \{x_1^0 x_n^0, \ldots, x_1^{n_1} x_n^{n_n}\}$. Applying $\mathfrak{D}_b$, we have $\mathfrak{D}_b(x_1^{j_1}x_n^{j_n}) = \{\zeta_{j+j_1}x_n^{j_n-1}\}_{j=1}^{P}$. As before, iterating the terms b and c together leads to $\mathfrak{D}_{\mathrm{b}}(V_{n+1}) \setminus V_{n+1} \subseteq \{x_1^0, \ldots, x_1^{n_1}\}$.

Hence, based on case n, we know that for $V_{n+1} \leftarrow V_{n+1} \cup \mathfrak{D}_{\mathrm{b}}(V_{n+1})$ taking $W_{n+1} = \{x_{n+1}\} \cup V_{n+1}$ and $\Phi = \mathrm{vec}(\bigcup_{i=1}^{n+1} W_i)$ will ensure that condition (8a) holds true. This completes the proof.

This shows that for an autonomous polynomial nonlinear system with dynamics described by (10), there exists a finite dimensional lifting Φ, containing the states and polynomial terms, satisfying $\dot{\Phi} = \frac{\partial \Phi}{\partial x} f \in \mathrm{span}\{\Phi\}$. This implies that there exists a square real matrix A such that $\dot{\Phi}(x) = A\Phi(x)$.

2.3 Systems with input

Next, we present the extension to systems with inputs. Consider the following control affine nonlinear system:

$$\dot{x} = f(x) + g(x)u, \tag{23}$$

with the autonomous part given by (10) and $g : \mathbb{R}^{n_\mathrm{x}} \to \mathbb{R}^{n_\mathrm{x} \times n_\mathrm{u}}$ and $u \in \mathbb{U} \subseteq \mathbb{R}^{n_\mathrm{u}}$. To obtain the lifted representation, one can use the sequential method described in (Iacob et al., 2022). First, an exact lifting of the autonomous part is computed such that conditions (8) hold. Next, the Koopman embedding is computed using the properites of the differential operator. Applying the lifting Φ and taking the time derivative, one obtains:

$$\begin{aligned} \dot{\Phi} &= \frac{\partial \Phi}{\partial x}(x)\dot{x} \\ &= \frac{\partial \Phi}{\partial x}(x)f(x) + \frac{\partial \Phi}{\partial x}(x)g(x)u. \end{aligned} \tag{24}$$

Using the equivalence of conditions (8b) and (8a), an associated Koopman embedding of (23) is:

$$\dot{\Phi}(x) = A\Phi(x) + B(x)u, \tag{25}$$

with $B(x) = \frac{\partial \Phi}{\partial x}(x)g(x)$. As described in (Iacob et al., 2022), one can further express (25) as a *linear parameter varying* (LPV) Koopman form by introducing a scheduling map $p = \mu(z)$, where $z = \Phi(x)$ and defining $B_\mathrm{z} \circ z = B$. Then, the LPV Koopman model is described by:

$$\dot{z} = Az + B_\mathrm{z}(p)u, \tag{26}$$

with $z(0) = \Phi(x(0))$.

Moreover, as shown in (Goswami and Paley, 2017; Iacob et al., 2022), if $\frac{\partial \Phi}{\partial x} g_i \in \mathrm{span}\{\Phi\}$ (g_i is the i^{th} column of g), then there is a matrix $B_i \in \mathbb{R}^{n_\mathrm{f} \times n_\mathrm{f}}$ that satisfies:

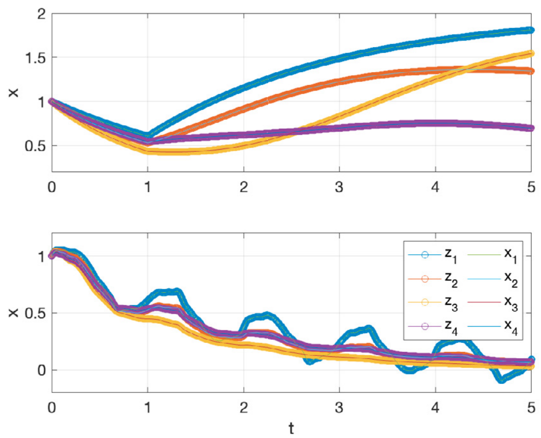

Fig. 3. State trajectories of the original nonlinear system detailed in Section 3.2 and the Koopman embedding (31) under step (top) and multisine inputs (bottom).

$$\frac{\partial \Phi}{\partial x} g_i = B_i \Phi. \tag{27}$$

As such, the lifted model can be written in a bilinear form:

$$\dot{z} = Az + \sum_{i=1}^{n_\mathrm{u}} B_i z u_i, \tag{28}$$

where u_i is the i^{th} component of u and $z = \Phi(x)$. Note that different equivalent bilinear models can be formulated as detailed in (Iacob et al., 2022).

3. EXAMPLE

This section presents the embedding of a 4-dimensional system and shows simulation results for both autonomous and input-driven operation.

3.1 Autonomous case

Consider the following 4th order system:

$$\dot{x}_1 = a_1 x_1 \tag{29a}$$
$$\dot{x}_2 = a_2 x_2 + \alpha_3^2 x_1^3 \tag{29b}$$
$$\dot{x}_3 = a_3 x_3 + \alpha_{11}^3 x_1 x_2 + \alpha_{02}^3 x_2^2 \tag{29c}$$
$$\dot{x}_4 = a_4 x_4 + \alpha_{111}^4 x_1 x_2 x_3. \tag{29d}$$

We can apply the procedure discussed in Section 2 per state equation to find the observable functions. The resulting lifting functions are as follows: $W_1 = \{x_1\}$, $W_2 = \{x_2, x_1^3\}$, $W_3 = \{x_3, x_1x_2, x_2^2, x_1^4, x_1^3x_2, x_1^6\}$, and $W_4 = \{x_4, x_1x_2x_3, x_1^4x_3, x_1^2x_2, x_1x_2^3, x_1^5x_2, x_1^4x_2, x_1^8, x_1^7x_2, x_1^{10}\}$.

The entire lifting set is $\Phi = \mathrm{vec}(W_1, W_2, W_3, W_4)$. For easier interpretability, we write the observables as $\Phi(x) = [x_1\ x_2\ x_3\ x_4\ \bar{\Phi}_1^\top\ \bar{\Phi}_2^\top\ \bar{\Phi}_3^\top\ \bar{\Phi}_4^\top]^\top$ where $\bar{\Phi}_i$ contains the elements of W_i, in order, without the state x_i. Performing the derivations as described in the proof, we obtain a finite dimensional Koopman representation of the form:

$$\dot{z} = Az, \quad x = Cz, \tag{30}$$

with $z(t) = \Phi(x(t))$, $A \in \mathbb{R}^{19\times 19}$ and $C = [I_4\ 0_{4\times 15}]$. The structure of the state matrix A is detailed in the Appendix. To compare the Koopman representation and the original system description, let $a_1 = a_2 = a_3 = a_4 = -0.5$, $\alpha_3^{(2)} = \alpha_{11}^{(3)} = \alpha_{02}^{(3)} = \alpha_{111}^{(4)} = -0.2$ and $x_0 = [1\ 1\ 1\ 1]^\top$. We can obtain solution trajectories of these two representations by a Runge-Kutta 4th-order solver. Furthermore, once the initial condition is lifted, i.e. $z(0) = \Phi(x(0))$, the dynamics of the Koopman model are driven forward linearly, as described by (30). Simulation results of the Koopman model and the original nonlinear representation from a given initial condition are depicted in Fig 1. As it can be observed, there is an exact overlap between the state trajectories of the original system description and the state trajectories obtained from the lifted model ($z_{1\to 4}$ correspond to $x_{1\to 4}$). Fig. 2 shows that the obtained error is in the order of magnitude of 10^{-15}, which can be attributed to numerical artifacts.

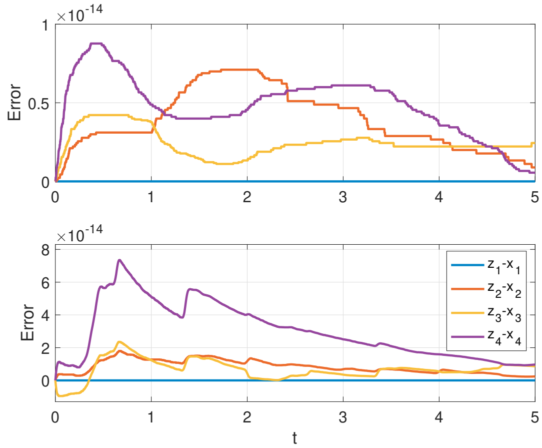

Fig. 4. Error between the state trajectories of the original nonlinear system detailed in Section 3.2 and the Koopman embedding (31) under under step (top) and multisine inputs (bottom).

3.2 Input-driven case

Consider a control affine nonlinear system (23), with the autonomous part given by the equations (29a)-(29d) and $g(x) = \left[1\ x_1\ x_2^2\ \sin(x_3)\right]^\top$. Applying the lifting procedure described in Section 2.3, we can derive an exact LPV Koopman model:

$$\dot{z} = Az + B_\mathrm{z}(p)u \tag{31a}$$
$$x = Cz, \tag{31b}$$

with $C = [I_4\ 0_{4\times 15}]$, $z(t) = \Phi(x(t))$ and $p = z$. Note that the state matrix A coincides with the autonomous case. The explicit form of $B(x)$ (and, in turn, B_z) is omitted due to space constraints, but it can be easily computed by multiplying $\frac{\partial \Phi}{\partial x}$ with $g(x)$. The structure of $\frac{\partial \Phi}{\partial x}(x)$ is given in the Appendix. We use the same coefficient values as in the autonomous case. After lifting the initial state $z(0) = \Phi(x(0))$, the dynamics of the Koopman representation are simulated forward in time by (31) for a step input (at time $t = 1$) and a multisine input with excited frequencies placed equidistantly between 1 and 10 Hz with no phase difference. Fig. 3 shows the solution trajectories of both the original and the lifted system representations. There is an exact overlap, i.e., the error of the state trajectories, depicted in Fig. 4, is in the magnitude of 10^{-14}, which is due to numerical integration.

4. CONCLUSIONS

The present paper shows that a finite, exact Koopman embedding exists for a specific system class and an approach is provided to obtain this embedding. Furthermore, as shown, the step to embed nonlinear systems with input is easily achieved once the autonomous part is lifted. Future work will focus on extending the current system description to a more general class of nonlinear systems.

5. APPENDIX

$$A = \begin{bmatrix}
a_1 & 0 & 0 & 0 & 0 & 0 & 0 & 0 & 0 & 0 & 0 & 0 & 0 & 0 & 0 & 0 & 0 & 0 & 0 \\
0 & a_2 & 0 & 0 & \alpha_3^{(2)} & 0 & 0 & 0 & 0 & 0 & 0 & 0 & 0 & 0 & 0 & 0 & 0 & 0 & 0 \\
0 & 0 & a_3 & 0 & 0 & \alpha_{11}^{(3)} & \alpha_{02}^{(3)} & 0 & 0 & 0 & 0 & 0 & 0 & 0 & 0 & 0 & 0 & 0 & 0 \\
0 & 0 & 0 & a_4 & 0 & 0 & 0 & 0 & 0 & 0 & \alpha_{111}^{(4)} & 0 & 0 & 0 & 0 & 0 & 0 & 0 & 0 \\
0 & 0 & 0 & 0 & 3a_1 & 0 & 0 & 0 & 0 & 0 & 0 & 0 & 0 & 0 & 0 & 0 & 0 & 0 & 0 \\
0 & 0 & 0 & 0 & 0 & a_1+a_2 & 0 & \alpha_3^{(2)} & 0 & 0 & 0 & 0 & 0 & 0 & 0 & 0 & 0 & 0 & 0 \\
0 & 0 & 0 & 0 & 0 & 0 & 2a_2 & 0 & 2\alpha_3^{(2)} & 0 & 0 & 0 & 0 & 0 & 0 & 0 & 0 & 0 & 0 \\
0 & 0 & 0 & 0 & 0 & 0 & 0 & 4a_1 & 0 & 0 & 0 & 0 & 0 & 0 & 0 & 0 & 0 & 0 & 0 \\
0 & 0 & 0 & 0 & 0 & 0 & 0 & 0 & 3a_1+a_2 & \alpha_3^{(2)} & 0 & 0 & 0 & 0 & 0 & 0 & 0 & 0 & 0 \\
0 & 0 & 0 & 0 & 0 & 0 & 0 & 0 & 0 & 6a_1 & 0 & 0 & 0 & 0 & 0 & 0 & 0 & 0 & 0 \\
0 & 0 & 0 & 0 & 0 & 0 & 0 & 0 & 0 & 0 & a_1+a_2+a_3 & \alpha_3^{(2)} & \alpha_{11}^{(3)} & \alpha_{02}^{(3)} & 0 & 0 & 0 & 0 & 0 \\
0 & 0 & 0 & 0 & 0 & 0 & 0 & 0 & 0 & 0 & 0 & 4a_1+a_3 & 0 & 0 & \alpha_{11}^{(3)} & \alpha_{02}^{(3)} & 0 & 0 & 0 \\
0 & 0 & 0 & 0 & 0 & 0 & 0 & 0 & 0 & 0 & 0 & 0 & 2a_1+2a_2 & 0 & 2\alpha_3^{(2)} & 0 & 0 & 0 & 0 \\
0 & 0 & 0 & 0 & 0 & 0 & 0 & 0 & 0 & 0 & 0 & 0 & 0 & a_1+3a_2 & 0 & 3\alpha_3^{(2)} & 0 & 0 & 0 \\
0 & 0 & 0 & 0 & 0 & 0 & 0 & 0 & 0 & 0 & 0 & 0 & 0 & 0 & 5a_1+a_2 & 0 & \alpha_3^{(2)} & 0 & 0 \\
0 & 0 & 0 & 0 & 0 & 0 & 0 & 0 & 0 & 0 & 0 & 0 & 0 & 0 & 0 & 4a_1+2a_2 & 0 & 2\alpha_3^{(2)} & 0 \\
0 & 0 & 0 & 0 & 0 & 0 & 0 & 0 & 0 & 0 & 0 & 0 & 0 & 0 & 0 & 0 & 8a_1 & 0 & 0 \\
0 & 0 & 0 & 0 & 0 & 0 & 0 & 0 & 0 & 0 & 0 & 0 & 0 & 0 & 0 & 0 & 0 & 7a_1+a_2 & \alpha_3^{(2)} \\
0 & 0 & 0 & 0 & 0 & 0 & 0 & 0 & 0 & 0 & 0 & 0 & 0 & 0 & 0 & 0 & 0 & 0 & 10a_1
\end{bmatrix}$$

$$\frac{\partial \Phi}{\partial x}(x) = \begin{bmatrix}
1 & 0 & 0 & 0 & 3x_1^2 & x_2 & 0 & 4x_1^3 & 3x_1^2x_2 & 6x_1^5 & x_2x_3 & 4x_1^3x_3 & 2x_1x_2^2 & x_2^3 & 5x_1^4x_2 & 4x_1^3x_2^2 & 8x_1^7 & 7x_1^6x_2 & 10x_1^9 \\
0 & 1 & 0 & 0 & 0 & x_1 & 2x_2 & 0 & x_1^3 & 0 & x_1x_3 & 0 & 2x_1^2x_2 & 3x_1x_2^2 & x_1^5 & 2x_1^4x_2 & 0 & x_1^7 & 0 \\
0 & 0 & 1 & 0 & 0 & 0 & 0 & 0 & 0 & 0 & x_1x_2 & x_1^4 & 0 & 0 & 0 & 0 & 0 & 0 & 0 \\
0 & 0 & 0 & 1 & 0 & 0 & 0 & 0 & 0 & 0 & 0 & 0 & 0 & 0 & 0 & 0 & 0 & 0 & 0
\end{bmatrix}^\top$$

REFERENCES

Abraham, I. and Murphey, T.D. (2019). Active learning of dynamics for data-driven control using Koopman operators. *IEEE Transactions on Robotics*, 35(5), 1071–1083.

Bevanda, P., Sosnowski, S., and Hirche, S. (2021). Koopman operator dynamical models: Learning, analysis and control. *Annual Reviews in Control*, 52, 197–212.

Brunton, S.L., Budišić, M., Kaiser, E., and Nathan Kutz, J. (2022). Modern Koopman theory for dynamical systems. *SIAM Review*, 64, 229–340.

Cisneros, P.S.G., Datar, A., Göttsch, P., and Werner, H. (2020). Data-driven quasi-LPV model predictive control using Koopman operator techniques. *Proc. of the 21st IFAC World Congress*, 6062–6068.

Goswami, D. and Paley, D.A. (2017). Global bilinearization and controllability of control-affine nonlinear systems: A Koopman spectral approach. *Proc. of the 56th Annual Conference on Decision and Control*, 6107–6112.

Iacob, L.C., Beintema, G.I., Schoukens, M., and Tóth, R. (2021). Deep identification of nonlinear systems in Koopman form. *Proc. of the 60th IEEE Conference on Decision and Control*, 2288–2293.

Iacob, L.C., Tóth, R., and Schoukens, M. (2022). Koopman form of nonlinear systems with inputs. *arXiv:2207.12132.*

Jouan, P. (2003). Immersion of nonlinear systems into linear systems modulo output injection. *Proc. of the 42nd IEEE International Conference on Decision and Control*, 1476–1481.

Jungers, R.M. and Tabuada, P. (2019). Non-local linearization of nonlinear differential equations via polyflows. *Proc. of the American Control Conference*, 1906–1911.

Khalil, H.K. (2002). *Nonlinear systems; 3rd ed.* Prentice-Hall.

Klus, S., Nüske, F., Peitz, S., Niemann, J.H., Clementi, C., and Schütte, C. (2020). Data-driven approximation of the Koopman generator: Model reduction, system identification, and control. *Physica D: Nonlinear Phenomena*, 406, 132416.

Kowalski, K. and Steeb, W.H. (eds.) (1991). *Nonlinear Dynamical Systems and Carleman Linearization.* World Scientific.

Krener, A. and Isidori, A. (1983). Linearization by output injection and nonlinear observers. *Systems & Control Letters*, 3(1), 47–52.

Lasota, A. and Mackey, M.C. (1994). *Chaos, Fractals, and Noise: Stochastic Aspects of Dynamics.* Springer.

Lusch, B., Nathan Kutz, J., and Brunton, S. (2018). Deep learning for universal linear embeddings of nonlinear dynamics. *Nature Communications*, 9, 4950.

Mauroy, A., Mezić, I., and Susuki, Y. (eds.) (2020). *The Koopman Operator in Systems and Control: Concepts, Methodologies and Applications.* Springer.

Wang, Z. and Jungers, R. (2020). A data-driven immersion technique for linearization of discrete-time nonlinear systems. *Proc. of the 21st IFAC World Congress*, 869–874.

Williams, M., Kevrekidis, I., and Rowley, C. (2015). A data–driven approximation of the Koopman operator: Extending dynamic mode decomposition. *Journal of Nonlinear Science*, 25, 1307–1346.